Editors' Suggestion

# Relaxed Phase-Matching Constraints in Zero-Index Waveguides

Justin R. Gagnon,[1,†] Orad Reshef,[1,*,†] Daniel H. G. Espinosa,[2] M. Zahirul Alam,[1] Daryl I. Vulis,[3] Erik N. Knall,[3] Jeremy Upham,[1] Yang Li,[3,4] Ksenia Dolgaleva,[1,2] Eric Mazur,[3] and Robert W. Boyd[1,2,5]

[1]*Department of Physics, University of Ottawa, 25 Templeton Street, Ottawa, Ontario K1N 6N5, Canada*
[2]*School of Electrical Engineering and Computer Science, University of Ottawa, 25 Templeton Street, Ottawa, Ontario K1N 6N5, Canada*
[3]*John A. Paulson School of Engineering and Applied Sciences, Harvard University, 9 Oxford Street, Cambridge, Massachusetts 02138, USA*
[4]*State Key Laboratory of Precision Measurement Technology and Instrument, Department of Precision Instrument, Tsinghua University, 100084 Beijing, China*
[5]*Institute of Optics and Department of Physics and Astronomy, University of Rochester, 500 Wilson Blvd, Rochester, New York 14627, USA*

(Received 1 July 2021; accepted 4 April 2022; published 17 May 2022)

The utility of all parametric nonlinear optical processes is hampered by phase-matching requirements. Quasi-phase-matching, birefringent phase matching, and higher-order-mode phase matching have all been developed to address this constraint, but the methods demonstrated to date suffer from the inconvenience of only being phase matched for a single, specific arrangement of beams, typically copropagating, resulting in cumbersome experimental configurations and large footprints for integrated devices. Here, we experimentally demonstrate that these phase-matching requirements may be satisfied in a parametric nonlinear optical process for multiple, if not all, configurations of input and output beams when using low-index media. Our measurement constitutes the first experimental observation of direction-independent phase matching for a medium sufficiently long for phase matching to be relevant. We demonstrate four-wave mixing from spectrally distinct co- and counterpropagating pump and probe beams, the backward generation of a nonlinear signal, and excitation by an out-of-plane probe beam. These results explicitly show that the unique properties of low-index media relax traditional phase-matching constraints, which can be exploited to facilitate nonlinear interactions and miniaturize nonlinear devices, thus adding to the established exceptional properties of low-index materials.

DOI: 10.1103/PhysRevLett.128.203902

The nonlinear optical response of materials is the foundation upon which applications such as frequency conversion, all-optical signal processing, molecular spectroscopy, and nonlinear microscopy are built [1–4]. When light is generated by a parametric nonlinear interaction (e.g., harmonic generation [5]), the propagation direction of the generated output light is dictated by the properties of the input beams [6,7]. This dependence is due to conservation of momentum, also known as phase matching [6,8]. The amount by which the phase-matching condition is not satisfied is quantified by the phase mismatch $\Delta k$, the difference in the momentum of the constituent beams. Approaches such as quasi-phase-matching [9,10], birefringent phase matching [11], and higher-order-mode phase matching [12,13] have been demonstrated as means to achieve phase matching. However, these methods suffer from the inconvenience of only being phase matched for one specific configuration of the participating beams, which is typically collinear and along the direction of propagation [7], and only for a narrow range of wavelengths [14]. These constraints pose severe limitations on potential applications in nonlinear optics, where flexibility and compactness are highly desired.

There has been significant interest in using metamaterials to lift such constraints and explore the resulting novel behavior [7,14–19]. Metamaterials provide ultimate flexibility in the engineering of optical materials, enabling many unusual and interesting properties, including negative indices of refraction [20–22]. Materials with a negative refractive index have been used to demonstrate the second-harmonic generation of a nonlinear signal wave propagating against the pump wave, known as backward phase matching [14,23]. This unique behavior may be further explored when considering zero-index media [24,25].

As the magnitude of the momentum wave vector $k$ is proportional to the refractive index $n$ ($k = 2\pi n/\lambda$, where $\lambda$ is the free-space wavelength), it vanishes for light propagating in a zero-index medium. Consequently, light in a zero-index mode does not contribute any momentum to phase-matching considerations, and its propagation direction becomes inconsequential to the phase mismatch [Figs. 1(a) and 1(b)]. By virtue of this unique quality,

 © 2022 American Physical Society

many otherwise forbidden phenomena, such as the simultaneous generation of both forward- and backward-propagating light, become possible [7,26].

In our experiment, we explore these phenomena using Dirac-cone metamaterials that achieve an effective refractive index of zero via the simultaneous zero crossing of the permittivity and permeability, while maintaining a finite impedance [25,27]. These metamaterials consist of a pair of silicon-based, corrugated ridge waveguides whose dispersion profiles have zero crossings at 1600 or 1620 nm [27]. Figures 1(c) and 1(d) show an image of a fabricated waveguide and its measured refractive index profile. By sampling five distinct configurations of pump, signal, and idler waves, our experimental results support the existence of *direction-independent* phase matching.

In the four-wave mixing (FWM) interaction under investigation, a powerful pump beam interacts with a signal (probe) beam, converting two pump photons of frequency $\omega_p$ into one signal photon of frequency $\omega_s$ and one idler photon of frequency $\omega_i = 2\omega_p - \omega_s$ [28]. As is usually studied, all the beams of a FWM process are copropagating, and the phase mismatch is given by $\Delta k_{\mathrm{fw}} = 2k_p - k_s - k_i$,

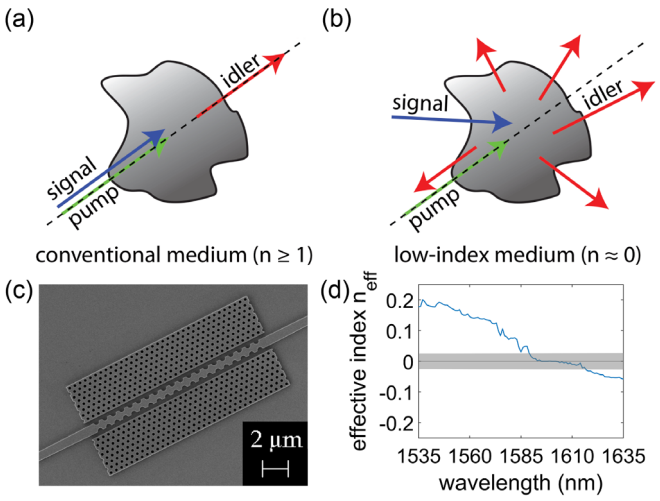


FIG. 1. Phase matching in a low-index medium. (a) In a conventional medium ($n > 1$), the input and output beams must be carefully aligned, typically copropagating, to satisfy the phase-matching condition. In a four-wave mixing interaction, this corresponds to aligning the signal beam with the pump beam to generate a collinear idler beam. (b) In a low-index medium ($n \approx 0$), the constituent beams are free to adopt any orientation and still maintain phase matching. (c) Scanning electron microscope image of a Dirac-cone zero-index waveguide surrounded by photonic band gap materials (triangular lattice of holes). (d) Refractive index profile of one of the waveguides used in the experiment, crossing zero at $\lambda = 1600$ nm. This refractive index profile was obtained via the method detailed in Ref. [27], whereby two counterpropagating beams are overlapped within the device and the resulting interference pattern is imaged from out of the plane. The shaded region indicates a refractive index below the measurement threshold of $n < 0.02$.

where suffixes $p$, $s$, and $i$ represent the pump, signal, and idler, respectively. In a standard silicon ridge waveguide, this phase-matching condition may be satisfied ($\Delta k \approx 0$). However, the phase mismatch would then prevent efficient FWM if the idler wave traveled in the backward direction (i.e., counterpropagating with respect to the pump beam), because then $\Delta k_{\mathrm{bw}} = 2k_p - k_s + k_i = \Delta k_{\mathrm{fw}} + 2k_i \approx 2k_i$. Similarly, phase mismatch would prevent efficient FWM if the signal wave was counterpropagating against the pump wave.

To explore the impact of a low-index response on phase matching, we consider the special case of copropagating input beams when the idler wave is generated at the zero-index wavelength. In this case, $\Delta k_{\mathrm{bw}} = \Delta k_{\mathrm{fw}} = 2k_p - k_s$, and any generated nonlinear forward- and backward-propagating signal would be expected to increase with equal efficiency due to the vanishing momentum contribution of $k_i$. In fact, for a given pump and signal wave configuration, generating an idler wave at the zero index is the sole condition under which the phase-matching condition can be satisfied multidirectionally for the idler wave due to $\Delta k_{\mathrm{bw}} = \Delta k_{\mathrm{fw}} + 2k_i$. Indeed, simulations predict that the backward-propagating idler wave is strongest when the idler is located at the zero-index wavelength.

The waveguides used in the experiment were fabricated by writing a pattern into a negative-tone resist using electron-beam lithography and subsequently transferring it to a silicon substrate using inductively coupled plasma reactive ion etching [27]. To facilitate coupling into the waveguides, polymer coupling pads with large cross-sectional areas were constructed on either end of the waveguide. The waveguides consist of a row of zero-index Dirac-cone metamaterial with a lattice constant of $a = 760$ nm, a cylindrical hole of radius $r = 212$ nm, and a thickness of 220 nm [27]. The waveguides are additionally bordered by a photonic band gap material consisting of a triangular lattice of holes with a lattice constant of 450 nm and a hole radius of 124 nm. These photonic band gap materials are used to reduce radiative losses in the waveguide [27]. The low dispersion in the waveguides, when combined with the effects of the vanishing refractive index, ensures that the phase mismatch is nearly zero for copropagating waves within a waveguide for the lengths being considered in this Letter, even when they are not located at the zero-index wavelength [27]. Two zero-index waveguides are used: waveguide A with a length of 14.8 $\mu$m and a zero-index wavelength of 1600 nm and waveguide B with a length of 11.1 $\mu$m with a zero-index wavelength of 1625 nm. The waveguides possess a refractive index of zero when using a transverse-electric polarization, and all three constituent beams of the FWM interaction use this mode. Their propagation loss has been previously determined to be wavelength dependent, with values of up to 1 dB/$\mu$m [27]. These loss values correspond largely to linear scattering losses, which far exceed

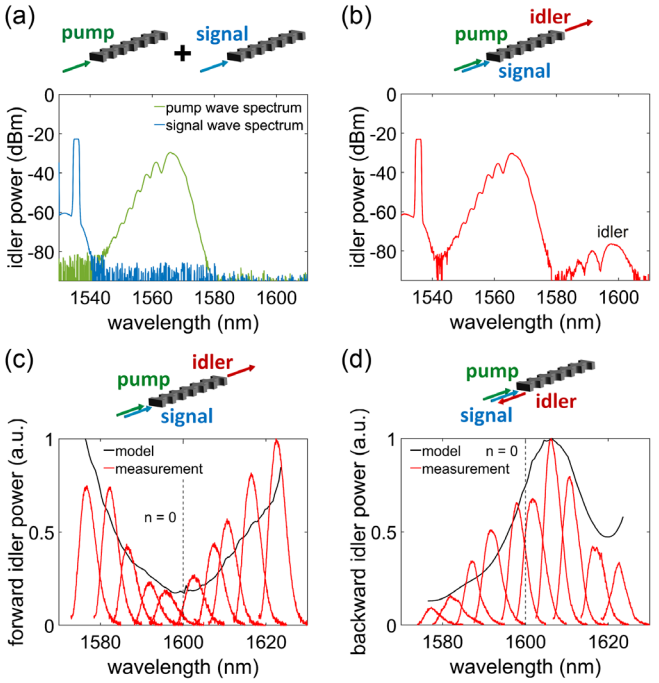


FIG. 2. Collinear phase-matching measurements. (a) Example spectra of the pump and signal waves when measured after propagating independently through a 14.8-$\mu$m-long low-index waveguide. (b) When these same pump and signal beams are simultaneously applied to the waveguide, an idler wave is generated in the forward direction at $\omega_i = 2\omega_p - \omega_s$ (1600 nm). The spectrum of the idler wave closely follows that of the pump wave because of the narrowness of the signal beam spectrum. Generated idler wave spectra in the (c) forward and (d) backward directions in a FWM process with copropagating pump and signal beams. The red curves show the spectra of the idler beams for ten different values of the pump and signal wavelengths. For each wavelength pair, the spectral gap between the pump and signal frequencies, as well as the incident power of the pump and signal beams, are held constant. The black curves show the peak power of the pulses predicted by phase-matching constraints, while the vertical dotted black lines in (c) and (d) indicate the $n = 0$ wavelength.

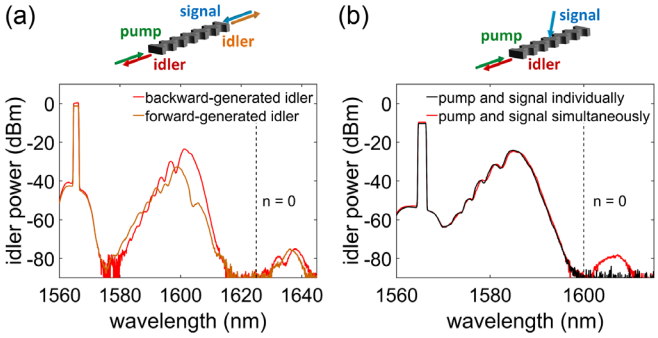


FIG. 3. Counterpropagating and out-of-plane phase-matching measurements. (a) Spectra showing FWM for counterpropagating pump and signal beams with an idler wave generated in the forward (copropagating with the pump wave, orange) and backward (copropagating with signal wave, red) directions. The signal and pump beams are at 1565 and 1600 nm, respectively, while the idler wave appears at 1635 nm. (b) Generated idler wave spectrum resulting from a signal beam seeding from out of the plane of the waveguide. An idler wave is generated in the backward direction only when the pump and signal beams are simultaneously applied (red curve compared to the black curve). The vertical dotted black lines in both figures indicate the $n = 0$ wavelength.

losses caused by two-photon absorption. We note that the two-photon absorption length of silicon for maximum pump intensity used in our experiment is 0.2 m, which far exceeds the nonlinear interaction lengths in our experiment [8,29,30]. Additional information concerning the structure of these waveguides can be found in Ref. [27]. Waveguide A is used for the copropagating and out-of-plane measurements [Figs. 2 and 3(b)]. However, in a setup featuring counterpropagating beams, there is less power overlap between the pump and signal beams due to propagation losses in the waveguide. As a result, waveguide B is used for the counterpropagating measurements [Fig. 3(a)] due to its shorter length, which allows for a larger power overlap.

In this experiment, a pulsed laser provides the pump beam, and an amplified continuous-wave laser provides the signal seed beam. The pulsed laser consists of a Ti:sapphire and optical parametric oscillator pumped by a 532 nm continuous-wave laser. This setup is capable of generating infrared pulses with a peak power of 1300 W, a pulse width of 3 ps, and a repetition rate of 76.3 MHz. The signal laser consists of a continuous-wave laser amplified by an erbium-doped fiber amplifier capable of accessing wavelengths between 1535 and 1565 nm with a peak power of 2 W. In measurements with copropagating beams involving a signal beam above 1565 nm, a weaker erbium-doped fiber amplifier capable of generating up to 100 mW was used. The spectra exiting the waveguide are measured using an optical spectrum analyzer set to a resolution of 2 nm.

To verify that phase-matching constraints are relaxed for multiple different orientations, we measure the output spectra from both ends of the waveguide when using three different pump and signal beam configurations: copropagating, counterpropagating, and with the signal beam seeding the waveguide from outside the beam plane. In our measurement with copropagating pump and signal beams, we sweep the pump wavelength in increments of 5 nm from 1555 to 1600 nm, while maintaining a constant spectral separation between the pump and signal waves ($\Delta f = c/\lambda_p - c/\lambda_s = 2.4$ THz). A constant spectral separation ensures dispersion will not contribute to any changes in the power of the generated idler waves. The power of the generated peaks has been shown to vary quadratically with the power of the pump wave; this dependence confirms that the peaks are the result of a FWM interaction. To ensure the effects of power are isolated, the incident power of the pump and signal is

additionally held constant. When the signal beam is incident on the sample from outside the beam plane, the measurements are performed with the pump wave at $\lambda = 1585$ nm and the signal wave at 1565 nm. As the waveguide will only accept light coming in at an incident angle defined by Snell's law and the refractive index at 1565 nm is slightly positive ($n \approx 0.17$), the signal beam is angled 9.8° off normal incidence, facing the pump beam. While there has been interest in enhanced nonlinearities of low-index media [25], we are not interested in the enhancement of generated nonlinear output in this Letter. Rather, our focus lies purely in studying the phase mismatch of the wave configurations.

As a first step toward demonstrating directionally unrestricted phase matching, we show the simultaneous generation of forward- and backward-propagating idler waves when considering the pump and signal beams copropagating in a waveguide (Fig. 2). Through the careful simultaneous adjustment of the pump and signal beams, this measurement produces idler waves for wavelengths of $\lambda_i$ ranging from 1570 to 1630 nm, crossing through the zero-index wavelength at $\lambda = 1600$ nm [Figs. 2(c) and 2(d)]. The backward-propagating light peaks at $\lambda_i = 1606$ nm, while the forward-propagating light has a dip centered at 1596 nm. We also plot our theoretical predictions alongside our experimental results [black curves in Figs. 2(c) and 2(d)]. The forward- and backward-generated spectra show almost perfect agreement with the theory in terms of both peak wavelength and rate of dropoff. The forward-generated idler wave dips in power shortly before the zero-index wavelength at 1596 nm. Modeling shows that this dip is caused by dispersive propagation loss and permeability values. Additionally, our model shows that the power of the backward-generated idler wave is comparatively much more heavily limited by the phase mismatch and, as a result, peaks when the backward-propagating idler wave is best phase matched [27]. Beyond the strong theoretical agreement, the fact that the most powerful backward-generated idler wave is not located at the same wavelength as the least powerful forward-generated idler wave constitutes additional proof that the backward-propagating idler wave is independently generated and does not merely consist of backscattering of the forward-propagating light due to possible reflections at the zero-index wavelength. Note that, in isolation, equal values of the generated idler powers are not a sufficient condition for claiming perfect phase matching. Indeed, there are many ways this could be otherwise achieved, such as with reflections or asymmetrical coupling efficiencies. However, the agreement with our model, which only considers the index, power, and loss as input parameters, proves that our observations arise from phase-matching constraints.

We next consider the phase-matching condition for other phase-matching configurations not possible in conventional waveguides. For counterpropagating pump and signal beams, simulations predict that the brightest forward-propagating idler wave will occur when the signal wave is at the zero-index wavelength (here at $\lambda = 1620$ nm), while for the backward-propagating idler wave it is predicted when the pump wave is at the zero-index wavelength. We perform measurements with a pump beam at 1600 nm and a signal beam at 1565 nm, where both requirements are best satisfied given experimental limitations. The resulting spectra are shown in Fig. 3(a). The simultaneous generation of forward- and backward-propagating idler waves is again clearly visible, here at $\lambda_i = 1630$ nm. The deviation in the shape of the generated idler wave spectra occurs due to spectral changes incurred by propagation in the waveguide, as well as fluctuations in the spectrum of the pump beam.

We further establish phase matching without directional restriction by coupling the pump beam into the waveguide as before and seeding the signal beam from outside the plane of the device. The seeding signal beam has a spot size diameter of 8 $\mu$m, corresponding to over half the length of the waveguide. A backward-propagating idler wave is observed at $\lambda_i = 1605$ nm as shown in Fig. 3(b). In addition to confirming our theoretical predictions, observing the FWM process from a signal beam seeding the waveguide from outside the plane of the device layer provides further proof that low-index waveguides significantly ease restrictions on parametric nonlinear effects by relaxing the phase-matching condition.

The simultaneous generation of forward- and backward-propagating idler light has been previously observed in a fishnet metamaterial with a total thickness of 800 nm [7]. However, the thickness of that metamaterial was smaller than the free-space optical wavelength ($\lambda = 1510$ nm) and phase mismatch is a smaller concern over such small propagation lengths [31]. Additionally, it would be very challenging to substantially increase the propagation length using this metamaterial platform. Consequently, it was difficult to establish that such an interaction would be phase matched over longer propagation distances. Our demonstration, in contrast, uses similar wavelengths in a 14.8-$\mu$m-long waveguide, corresponding to almost ten free-space optical wavelengths and consistent with a lower-bound estimate of the coherence length at 7.8 $\mu$m. Therefore, our low-index waveguides provide unambiguous proof that phase matching may be achieved for these longer distances, as opposed to the inference made in a thinner metasurface configuration. In addition, while this earlier demonstration used intrapulse FWM, our demonstration uses multiple spectrally distinct beams, enabling the clean isolation of the generated nonlinear pulses from the inputs, resulting in an unambiguous demonstration. These factors support the conclusion that the process is strongly phase matched. While our current zero-index platform exhibits radiative losses, theoretical estimates have been proposed to achieve low-loss zero-index waveguides, with propagation loss estimates of 15 [32], 10 [33], and 1.5 dB/cm [34]. More recent work has experimentally demonstrated several of

these designs [35], reporting a reduction of propagation loss by an order of magnitude compared to the waveguides in the present Letter.

In summary, we have experimentally demonstrated that a low-index medium enables phase matching that is free of directional restriction for the constituent beams, which greatly relaxes conventional nonlinear optical constraints and potentially enables all input and output beams to take on any desired configuration. Dirac-cone low-index waveguides can be constructed from any base material to enable these properties and could have a significant impact in several established and prospective technologies. In addition to facilitating the realization of FWM, this property can be used to facilitate other parametric nonlinear optical interactions. For example, in a difference-frequency generation interaction where $\omega_{\mathrm{DFG}} = \omega_p - \omega_s$, the phase-matching condition is given by $\Delta k = 0$, where $\Delta k = k_p - k_s \pm k_{\mathrm{DFG}}$. Therefore, if $k_{\mathrm{DFG}} = 0$, then when the condition of $n_p/\lambda_p - n_s/\lambda_s = 0$ is met, $k_{\mathrm{DFG}}$ can take any desired orientation. Furthermore, phase matching without directional restriction could be used to generate entangled idler photon pairs. While low-index materials still require conventional phase matching through the careful engineering of its dispersion parameter, they provide great flexibility in terms of propagation direction. We believe that such structured low-index media have the potential to facilitate the realization of nonlinear optical interactions due to the relaxation of this constraint and thus serve innumerable roles in the field of nonlinear optics.

Fabrication in this work was performed in part at the Center for Nanoscale Systems (CNS), a member of the National Nanotechnology Coordinated Infrastructure Network (NNCI), which is supported by the National Science Foundation under NSF Grant No. 1541959. CNS is part of Harvard University. The authors thank Kevin P. O'Brien for fruitful discussions. The authors gratefully acknowledge support from the Canada First Research Excellence Fund, the Canada Research Chairs Program, and the Natural Sciences and Engineering Research Council of Canada [NSERC (funding reference no. RGPIN/2017-06880)]. R. W. B. and E. M. acknowledge support from the Defense Advanced Research Projects Agency (DARPA) Defense Sciences Office (DSO) Nascent program and the U.S. Army Research Office. O. R. acknowledges the support of the Banting Postdoctoral Fellowship of the Natural Sciences. Portions of this work were presented at the 2016 Conference on Lasers and Electro-Optics (CLEO) in San Jose, CA [36].

J. R. G. carried out the nonlinear measurements. O. R. conceived the basic idea for this work. J. R. G., O. R., and D. H. G. E. designed the experiment. O. R. fabricated the devices. D. I. V. and E. K. carried out the linear measurements. O. R. and Y. L. carried out the simulations. J. R. G., O. R., J. U., and Z. A. analyzed the experimental results. R. W. B., J. U., E. M., and K. D. supervised the research and the development of the Letter. J. R. G. and O. R. wrote the first draft of the Letter, and all authors subsequently took part in the revision process and approved the final copy of the Letter.

*Corresponding author.
orad@reshef.ca
†J. R. G. and O. R. contributed equally to this work.

[1] E. Garmire, Opt. Express **21**, 30532 (2013).
[2] A. E. Willner, S. Khaleghi, M. R. Chitgarha, and O. F. Yilmaz, J. Lightwave Technol. **32**, 660 (2014).
[3] S. Mukamel, *Principles of Nonlinear Optical Spectroscopy* (Oxford University Press, New York City, NY, 1999).
[4] L. Schermelleh, R. Heintzmann, and H. Leonhardt, J. Cell Biol. **190**, 165 (2010).
[5] P. A. Franken, A. E. Hill, C. W. Peters, and G. Weinreich, Phys. Rev. Lett. **7**, 118 (1961).
[6] R. W. Boyd, *Nonlinear Optics*, 4th ed. (Academic Press, San Diego, California, 2020).
[7] H. Suchowski, K. O'Brien, Z. J. Wong, A. Salandrino, X. Yin, and X. Zhang, Science **342**, 1223 (2013).
[8] G. P. Agrawal, *Nonlinear Fiber Optics*, 4th ed. (Academic Press, Boston, MA, 2007).
[9] J. A. Armstrong, N. Bloembergen, J. Ducuing, and P. S. Pershan, Phys. Rev. **127**, 1918 (1962).
[10] M. Yamada, N. Nada, M. Saitoh, and K. Watanabe, Appl. Phys. Lett. **62**, 435 (1993).
[11] J. E. Midwinter and J. Warner, Br. J. Appl. Phys. **16**, 1135 (1965).
[12] C. C. Evans, K. Shtyrkova, O. Reshef, M. Moebius, J. D. B. Bradley, S. Griesse-Nascimento, E. Ippen, and E. Mazur, Opt. Express **23**, 7832 (2015).
[13] J. S. Levy, M. A. Foster, A. L. Gaeta, and M. Lipson, Opt. Express **19**, 11415 (2011).
[14] S. Lan, L. Kang, D. T. Schoen, S. P. Rodrigues, Y. Cui, M. L. Brongersma, and W. Cai, Nat. Mater. **14**, 807 (2015).
[15] K.-H. Luo, V. Ansari, M. Massaro, M. Santandrea, C. Eigner, R. Ricken, H. Herrmann, and C. Silberhorn, Opt. Express **28**, 3215 (2020).
[16] N. Voloch-Bloch, T. Davidovich, T. Ellenbogen, A. Ganany-Padowicz, and A. Arie, Opt. Lett. **35**, 2499 (2010).
[17] L. Planat, A. Ranadive, R. Dassonneville, J. Puertas Martinez, S. Leger, C. Naud, O. Buisson, W. Hasch-Guichard, D. M. Basko, and N. Roch, Phys. Rev. X **10**, 021021 (2020).
[18] N. Kinsey, C. DeVault, A. Boltasseva, and V. M. Shalev, Nat. Rev. Mater. **4**, 742 (2019).
[19] C. Wang, Z. Li, M.-H. Kim, X. Xiong, X.-F. Ren, G.-C. Guo, N. Yu, and M. Loncar, Nat. Commun. **8**, 2098 (2017).
[20] R. A. Shelby, D. R. Smith, and S. Schultz, Science **292**, 77 (2001).
[21] J. Valentine, S. Zhang, T. Zentgraf, E. Ulin-Avila, D. A. Genov, G. Bartal, and X. Zhang, Nature (London) **455**, 376 (2008).
[22] H. J. Lezec, J. A. Dionne, and H. A. Atwater, Science **316**, 430 (2007).

[23] L. Liu, L. Wu, J. Zhang, Z. Li, B. Zhang, and Y. Luo, Adv. Sci. **5**, 1800661 (2018).
[24] I. Liberal and N. Engheta, Nat. Photonics **11**, 149 (2017).
[25] D. I. Vulis, O. Reshef, P. Camayd-Muñoz, and E. Mazur, Rep. Prog. Phys. **82**, 012001 (2019).
[26] O. Reshef, I. De Leon, M. Z. Alam, and R. W. Boyd, Nat. Rev. Mater. **4**, 535 (2019).
[27] O. Reshef, P. Camayd-Muñoz, D. I. Vulis, Y. Li, M. Lončar, and E. Mazur, ACS Photonics **4**, 2385 (2017).
[28] M. A. Foster, A. C. Turner, J. E. Sharping, B. S. Schmidt, M. Lipson, and A. L. Gaeta, Nature (London) **441**, 960 (2006).
[29] A. T. Obeidat, W. H. Knox, and J. B. Khurgin, Opt. Express **1**, 68 (1997).
[30] G. W. Rieger, K. S. Virk, and J. Young, Appl. Phys. Lett. **84**, 900 (2004).
[31] M. Kauranen and A. Zayats, Nat. Photonics **6**, 737 (2012).
[32] P. Camayd-Munoz, S. Kita, O. Mello, O. Reshef, D. I. Vulis, Y. Li, M. Lončar, and E. Mazur, in *Conference on Lasers and Electro-Optics* (Optical Society of America, San Jose, CA, 2016), p. JW2A.24.
[33] M. Minkov, I. A. D. Williamson, M. Xiao, and S. Fan, Phys. Rev. Lett. **121**, 263901 (2018).
[34] T. Dong, J. Liang, S. Camayd-Muñoz, Y. Liu, H. Tang, S. Kita, P. Chen, X. Wu, W. Chu, E. Mazur, and Y. Li, Light **10**, 10 (2021).
[35] H. Tang, C. DeVault, S. A. Camayd-Muñoz, Y. Liu, D. Jia, F. Du, O. Mello, D. I. Vulis, Y. Li, and E. Mazur, Nano Lett. **21**, 914 (2021).
[36] O. Reshef, Y. Li, M. Yin, L. Christakis, D. I. Vulis, P. C.-M. noz, S. Kita, M. Lončar, and E. Mazur, in *Conference on Lasers and Electro-Optics* (Optical Society of America, San Jose, CA, 2016).
[37] See Supplemental Material at http://link.aps.org/supplemental/10.1103/PhysRevLett.128.203902 for some theoretical modeling, an overview of Dirac-cone metamaterials, simulation results, discussions on conversion efficiencies, estimates on the coherence length, the waveguide dispersion, a description of the experimental setup, and the power dependencies on the generated idler, which also includes Refs. [38–49].
[38] N. Mattiucci, G. D'Aguanno, M. Scalora, and M. J. Bloemer, J. Opt. Soc. Am. B **24**, 877 (2007).
[39] J. D. Joannopoulos, S. G. Johnson, J. N. Winn, and R. D. Meade, *Photonic Crystals—Molding the Flow of Light*, 2nd ed. (Princeton University Press, Princeton, New Jersey, 2007).
[40] X. Huang, Y. Lai, Z. H. Hang, H. Zheng, and C. T. Chan, Nat. Mater. **10**, 582 (2011).
[41] K. Sakoda, J. Opt. Soc. Am. B **29**, 2770 (2012).
[42] K. Sakoda, Opt. Express **20**, 3898 (2012).
[43] S. Kita, Y. Li, P. Camayd-Muñoz, O. Reshef, D. I. Vulis, R. W. Day, E. Mazur, and M. Lončar, Opt. Express **25**, 8326 (2017).
[44] Y. Wu, J. Li, Z.-Q. Zhang, and C. T. Chan, Phys. Rev. B **74**, 085111 (2006).
[45] D. I. Vulis, Y. Li, O. Reshef, P. Camayd-Muñoz, M. Yin, S. Kita, M. Loncar, and E. Mazur, Opt. Express **25**, 12381 (2017).
[46] O. Reshef, Integrated metamaterials and nanophotonics in CMOS-compatible materials, Ph.D. thesis, Harvard University, 2016, http://nrs.harvard.edu/urn-3:HUL.InstRepos:33840733.
[47] K. O'Brien, H. Suchowski, J. Rho, A. Salandrino, B. Kante, X. Yin, and X. Zhang, Nat. Mater. **14**, 379 (2015).
[48] M. Pu, H. Hu, L. Ottaviano, E. Semenova, D. Vukovic, L. Oxenlowe, and K. Yvind, Laser Photonics Rev. **12**, 1800111 (2018).
[49] D. H. Espinosa, K. M. Awan, M. Odungide, S. R. Harrigan, D. R. Sanchez, and K. Dolgaleva, Opt. Commun. **479**, 126450 (2021).